Appl Phys B
DOI 10.1007/s00340-011-4435-1

Volume 103, Number 1, 27-33 (2011), DOI: 10.1007/s00340-011-4435-1

Applied Physics B
Lasers and Optics

Compact all-solid-state continuous-wave single-frequency UV source with frequency stabilization for laser cooling of Be^+ ions

S. Vasilyev · A. Nevsky · I. Ernsting · M. Hansen · J. Shen · S. Schiller

Received: 26 October 2010 / Revised version: 13 December 2010

Abstract A compact setup for generation, frequency stabilization, and precision tuning of UV laser radiation at 313 nm was developed. The source is based on frequency quintupling of a C-band telecom laser at 1565 nm, amplified in a fiber amplifier. The maximum output power of the source at 313 nm is 100 mW. An additional feature of the source is the high-power output at the fundamental and the intermediate second- and third-harmonic wavelengths. The source was tested by demonstration of laser cooling of Be^+ ions in an ion-trap apparatus. The output of the source at the third-harmonic wavelength (522 nm) was used for stabilization of the laser frequency to molecular iodine transitions. Sub-Doppler spectroscopy and frequency measurements of hyperfine transitions in molecular iodine were carried out in the range relevant for the Be^+ laser cooling application.

1 Introduction

Single-frequency UV laser sources are used in a variety of research related to high-resolution spectroscopy of atoms, molecules and ions. As an example from quantum optics, the beryllium ion, laser cooled on the $2s \rightarrow 2p$ transition at a wavelength of 313 nm, is a workhorse of quantum computing, precision spectroscopy of atomic and molecular ions via sympathetic cooling, and of the quantum logic optical clock [1–5], and is of interest for the nuclear structure of its isotopes [6, 7]. The UV laser source required for such experiments should be as simple, reliable, and compact as possible, so as to keep the complexity of the experiments manageable.

Single-frequency lasers directly emitting at wavelengths around 313 nm do not exist. Second-harmonic generation (SHG) of a dye laser at 626 nm is a straightforward solution but is expensive. Sum-frequency generation (SFG) of a Ti:Sapphire laser (650–1100 nm) and a frequency doubled Nd-doped laser (532 nm) allows one to cover the UV range between 293 and 358 nm using SFG in LBO or BBO nonlinear crystals. Such a source, employing SFG in a doubly-resonant enhancement cavity has been previously developed and used for Be^+ cooling [8]. Similar to the dye laser solution, the drawbacks of this approach are high initial and maintenance costs of the lasers, high complexity and bulkiness of the optical setup, the necessity to stabilize the frequency of two laser sources.

A much simpler and cost-efficient all-solid-state solution is SHG of diode-laser (DL) emission. This approach became of practical use with an advent of high-power DL amplifiers. UV laser sources based on frequency doubling or quadrupling of DL MOPAs (master oscillator power amplifier) are now commercially available. Unfortunately, the 313 nm wavelength cannot be addressed in this way for lack of DLs with reasonably high power at subharmonic wavelengths of 626 nm and 1252 nm. A feasible solution is using a 939 nm DL MOPA, followed by SHG and SFG stages. However the UV output power from such a system would be much lower than that from the system described below.

Due to remarkable progress in the fiber laser technology, reliable and cost-efficient near-IR fiber lasers and amplifiers with high spectral purity and high output power are now available [9, 10]. Currently, high-power cw ytterbium (Yb) and erbium (Er) doped fiber lasers are used success-

S. Vasilyev (✉) · A. Nevsky · I. Ernsting · M. Hansen · J. Shen · S. Schiller
Institut für Experimentalphysik, Heinrich-Heine-Universität Düsseldorf, Universitätsstr. 1, 40225 Düsseldorf, Germany
e-mail: Sergey.Vasilyev@uni-duesseldorf.de
url: http://www.exphy.uni-duesseldorf.de
Fax: +49-211-8113116

Published online: 26 February 2011

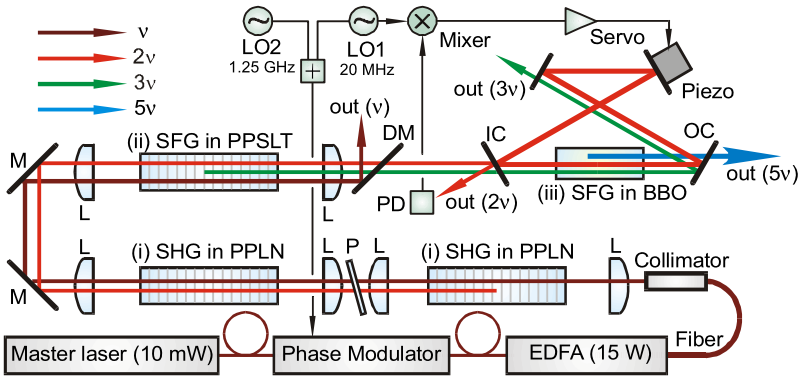

Fig. 1 Schematic of the setup for frequency quintupling of the 1565 nm laser. L: lenses, M: mirrors, DM: dichroic mirror, P: Brewster plate for phase mismatch compensation (see text), IC/OC: input and output couplers of the enhancement cavity PD: photodetector, out (ν, 2ν, 3ν, 5ν): output beams at fundamental, second, third and fifth-harmonic wavelength. The third-harmonic output, out (3ν) is delivered to the frequency stabilization system (see Sect. 3)

fully as a starting point for a various kinds of nonlinear frequency conversion [11–14]. The high (and easily scalable) fiber laser power can be combined with the performance of modern nonlinear materials based on quasi-phase-matching (QPM). First commercial systems for nonlinear frequency conversion of fiber lasers are appearing.

By a convenient coincidence, the 313 nm UV wavelength, relevant for Be^+ cooling, is a fifth harmonic of the 1565 nm IR wavelength, which is within the range of the Er-doped fiber lasers, and within the C-band of fiber-optic communication. Consequently a variety of active and passive components are mass produced and easily available for this wavelength.

An apparent drawback of the UV generation by quintupling of the 1565 nm radiation, is the relatively large number of nonlinear frequency conversion stages, and hence the relatively low overall conversion efficiency. However, this can be compensated by increase (at a reasonable cost) of the fiber laser power at the fundamental wavelength.

In this paper we report on a UV source based on quintupling of the IR laser and suitable for laser cooling of Be^+ ions. A narrowband telecom laser is amplified to 15 W in an Er-doped fiber amplifier (EDFA) and then the fifth harmonic (5H) of the fundamental frequency is generated in a chain of nonlinear crystals. The main advantage of the source is the compact and robust design, owing to the reliability of the fiber laser components. The footprint of the quintupling setup is less than 0.2 m^2, where the seed laser at the fundamental wavelength, the EDFA, and the auxiliary fiber components can be located in a rack rather than on the optical table. A UV output power of 100 mW was reached using an enhancement cavity in the last frequency conversion stage. A UV power of 2 mW was measured without the enhancement cavity, i.e. using an all-single-pass configuration of the frequency conversion setup. This simplified source is especially robust and can be used for less power demanding applications.

The intermediate third-harmonic output of the source (522 nm) provides a convenient means for laser frequency stabilization since molecular iodine is an excellent and well-studied reference for laser wavelengths in the green. We implemented a system for frequency stabilization and precision tuning of the UV output frequency around the Be^+ cooling transition. The frequency of the UV source can be stabilized to various hyperfine components in the spectrum of molecular iodine and in addition can be continuously and precisely offset-tuned by a double-pass AOM frequency shifter.

The developed UV source was integrated in our experimental apparatus for laser cooling of Be^+ ions and sympathetic cooling of molecular ions and was successfully tested during long-term (multi-hour) experiments.

2 Nonlinear frequency conversion setup

The schematic of the setup for frequency quintupling of the infrared laser at 1565 nm is shown in Fig. 1. A master laser, a single-frequency Er-doped distributed-feedback (DFB) fiber laser module (Koheras K80-153-12), was amplified in a 15-W polarization-maintaining EDFA (IPG EAR-15K-C-LP-SF-UD). A fiber-optic phase modulator was placed in-between the master laser and the amplifier to produce two sets of sidebands, used for the enhancement cavity locking (modulation frequency: 20 MHz), and for producing a Be^+ repumper wave (modulation frequency: 1.25 GHz).

Frequency conversion of the fundamental laser frequency (ν) to the fifth harmonic (5ν) was realized in the following stages: (i) single-pass SHG ($\nu + \nu \rightarrow 2\nu$) in a cascade of two 50-mm long periodically poled lithium niobate crystals (PPLN, Deltronic); (ii) single-pass SFG ($\nu + 2\nu \rightarrow 3\nu$) in the 30-mm long periodically poled magnesium doped lithium tantalate crystal (PPSLT, HCP); (iii) SFG ($2\nu + 3\nu \rightarrow 5\nu$) in a 10-mm long BBO crystal (Ekspla). The BBO crystal was placed in the enhancement cavity in order to increase the UV output power (this frequency conversion stage can also be of single-pass type, for low-power applications). All nonlinear crystals were temperature stabilized

within 0.1°C. Simple plano-convex (PCX) lenses were used for the beam focusing and collimation.

In our opinion, the chosen sequence of frequency conversions and of the intermediate wavelengths is well balanced. The PPLN and PPSLT crystals are resistant to "photorefractive damage" under high-power irradiation at intermediate second- and third-harmonic wavelengths. The third-harmonic output at 522 nm can be used for frequency stabilization of the source, as will be discussed below. The overall optical design of the source is rather simple and hence robust. All frequency conversions but one are of single-pass type and no laser beam combining is needed. The use of the single-pass arrangement with very efficient QPM nonlinear crystals, in combination with the cavity-enhanced arrangement for the BBO crystal, is a good compromise between simplicity and performance of the UV source. The footprint of the frequency conversion setup is 0.6 m × 0.3 m and could be further reduced.

The first (SHG) step of frequency conversions is done in a cascade of two nonlinear crystals [15]. Theoretically, this provides up to a factor 4 increase of the SHG efficiency. Dispersion in the refocusing lenses in-between the two crystals and in the air introduces a phase mismatch between the fundamental and the second-harmonic waves at the front end of the second crystal in the cascade. A Brewster plate (P in Fig. 1) was used in the setup to compensate and adjust the phase mismatch (e.g. a 1° tilt of the 3-mm thick glass plate corresponds to a π phase shift between the two waves while the chromatic aberration introduced by the plate is minuscule).

The measured second-harmonic (SH) power at the output of the cascade as a function of laser power at fundamental wavelength (pump, 1565 nm) is shown in Fig. 2a (left vertical axis). The maximum SH power of 7.7 W corresponds to 53% pump conversion efficiency. The dashed curve on the plot (right vertical axis) illustrates the enhancement of the SH power in the cascade with respect to the single-crystal SHG. Use of the cascade results in 330% SHG enhancement at low pump power. The difference between measured value and the theoretical limit (400%) can be explained by chromatic aberrations of the PCX lenses that were used for the refocusing. The decrease of the enhancement factor with increase of the pump power can be attributed to the various power-induced wavefront distortions and to the pump depletion. The measured output power of the source at the third-harmonic (TH) wavelength is shown in Fig. 2b by the green curve (left vertical axis). At 15 W pump power, 1.2 W TH output and 8% conversion efficiency were reached.

For the resonant SFG, we used a standard bow-tie enhancement cavity, with two plane and two curved mirrors (50 mm radii of curvature). A plane-parallel cut and antireflection-coated BBO crystal was located between the curved mirrors in the 30 μm waist of the cavity mode. The

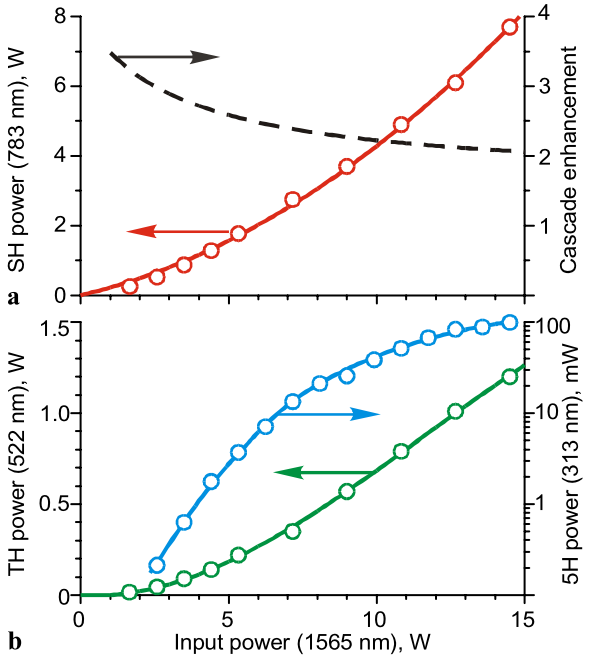

Fig. 2 Output power of the source at second, third and fifth-harmonic wavelength (SH, TH, 5H, respectively) vs. input power at fundamental wavelength. Part (**a**): *left axis*—SH power, *right axis*—enhancement factor of the two-crystal cascade (see text). Part (**b**): *left axis*—TH power, *right axis*—5H power (1 minute average) in logarithmic scale

cavity was designed to resonate with only one of the two input waves, the second harmonic at 783 nm. The third harmonic traverses the crystal in a single pass and then is being delivered to the frequency stabilization system (see Fig. 1). This arrangement was chosen to minimize the interference between the enhancement cavity and the frequency stabilization system, which relies on the third-harmonic output (i.e. the enhancement cavity and the laser frequency can be scanned and locked independently).

The cavity was locked to the master laser using the standard Pound–Drever–Hall (PDH) technique [16, 17]. The sidebands for the PDH lock (20 MHz) we generated in the fiber-optic phase modulator. The modulator was placed between the master laser and the EDFA (see Fig. 1) and modulates the fundamental wave. The sidebands are maintained during the frequency conversions, as the phase-matching bandwidths of the nonlinear crystals are large enough.

The dependence of the UV fifth-harmonic (5H) output power on the input pump power is shown in Fig. 2b by the blue curve (right vertical axis). A logarithmic scale is used to make the plot more illustrative. As can be seen, the considerable level of 100 mW 5H output has been reached. Comparison with the 2 mW power measured for the single-pass conversion in the BBO crystal, shows that the enhancement factor of approx. 50 was obtained by using the enhancement cavity approach.

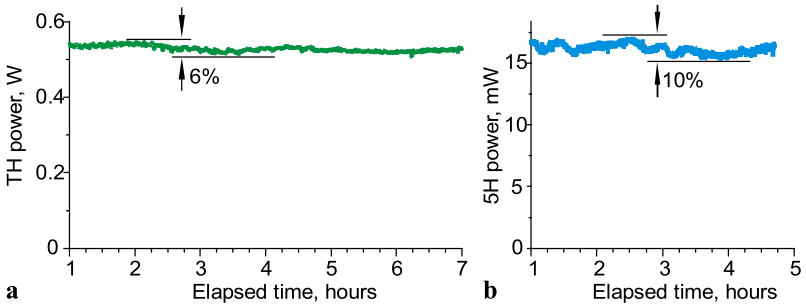

Fig. 3 Output power of the source at third-harmonic (TH) and fifth-harmonic (5H) wavelengths during long-term operation. Both measurements were started after 1 hour warming up of the setup

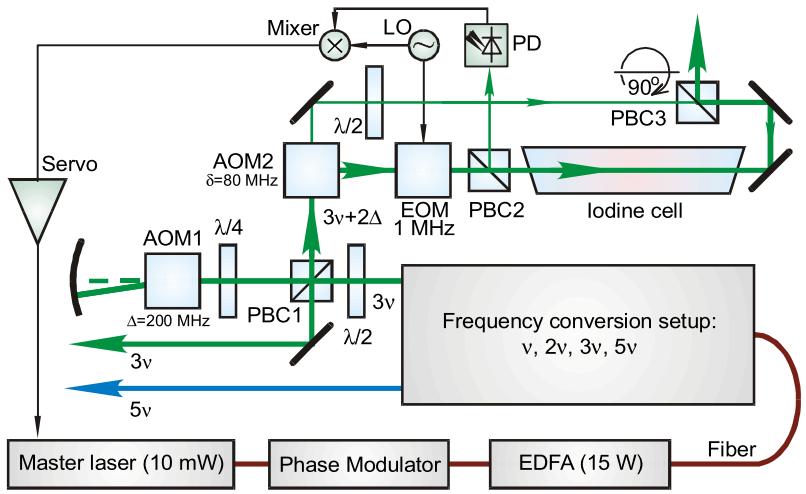

Fig. 4 Schematic of the setup for frequency stabilization and tuning of the UV source. 3ν, 5ν are the output beams at third and fifth-harmonic wavelength, PBC polarization beam splitter cubes (the PBC3 is rotated by 90° with respect to the PBC2, to reflect the pump beam and transmit the probe beam), $\lambda/2$, $\lambda/4$ wave plates, AOM acoustooptic modulators (AOM1 is used for fine frequency tuning), EOM: electrooptic modulator, PD: photodetector

The characterization of the power stability of the setup was carried out at a fundamental pump power reduced to 9 W. This pump power level corresponds to 15–20 mW 5H output power, which is more than sufficient for our Be^+ cooling setup. The output power stability at the TH wavelength is illustrated in Fig. 3a. The measurement was started after one hour warming up of the setup. The observed fluctuations of the TH power are mainly due to instability of the laser power at fundamental wavelength and due to temperature instabilities of the nonlinear crystals. No evidence of photorefractive damage of the QPM crystals was observed during the tests. No active control of the phase-matching between the fundamental and SH waves in the SHG cascade (adjustment of the plate P, see Fig. 1) was needed. Figure 3b shows the power stability of the fifth-harmonic UV output. This measurement was also started after one hour warming up. The observed fluctuations of the 5H power are within 10%.

If desired, the UV output power can be actively stabilized e.g. by polarization control of the fundamental wave, or by control of the phase shift in the SHG cascade (adjustment of the tilt of the plate P). Another, all-electronic, means for the power stabilization would be splitting of some laser power at fundamental wavelength from the central frequency to auxiliary sidebands, produced by the fiber-optic phase modulator (already included in the system).

The large margin of power (100 mW maximum output vs. several mW actually required for laser cooling applications) is an advantage in the practical use of the source. Temperature-induced misalignments and possible degradation of the BBO crystal and of other components can be compensated (to some extent) by an increase of the pump power at fundamental wavelength. Thus the source can be operated without maintenance during a longer time.

3 Frequency stabilization of the UV source

The frequency of the UV source was stabilized using molecular iodine as a reference. A schematic of the setup for frequency stabilization and tuning of the source is shown in Fig. 4. A fraction of the source's output at the third-harmonic wavelength (3ν) is split on the polarization beam splitter cube (PBC1) and sent to the double-pass acoustooptic frequency shifter (AOM1) with central frequency $\Delta = 200$ MHz and ± 50 MHz bandwidth. The frequency-shifted beam ($3\nu + 2\Delta$) is sent to the second AOM (AOM2 at 80 MHz) to produce the pump and the probe inputs for the Doppler-free frequency modulation transfer spectroscopy setup (FMTS, [18]) with the 15 cm long temperature stabilized iodine cell. The pump beam is modulated at 1 MHz by the electro optic modulator (EOM). The demodulated error

signal is fed back to the master laser via the servo amplifier. Thus the master laser's frequency can be locked to the hyperfine structure (hfs) components of molecular iodine transitions via the third-harmonic output of the source. The frequency of the fifth-harmonic UV output of the source (5ν) is related to the reference frequency of the hfs component (ν_{I2}) by the formula: $5\nu = (5/3) \cdot (\nu_{I2} - 2\Delta - \delta/2)$, where Δ is the modulation frequency of AOM1 and δ is the modulation frequency of AOM2. The UV output frequency can be fine-tuned by tuning the frequency Δ within the bandwidth of AOM1.

The absorption spectrum of molecular iodine in the wavelength range relevant for Be^+ cooling is shown in Fig. 5a. The measurement was carried out with the iodine cell at 10°C. The absorption lines were assigned using the atlas of Gerstenkorn and Luc [19]. By coincidence, the absorption line P58(2-49) is located rather close to the 521.888 nm TH wavelength (arrow on the plot), which corresponds to the 313.133 nm 5H UV wavelength (the Be^+ cooling transition [6]).

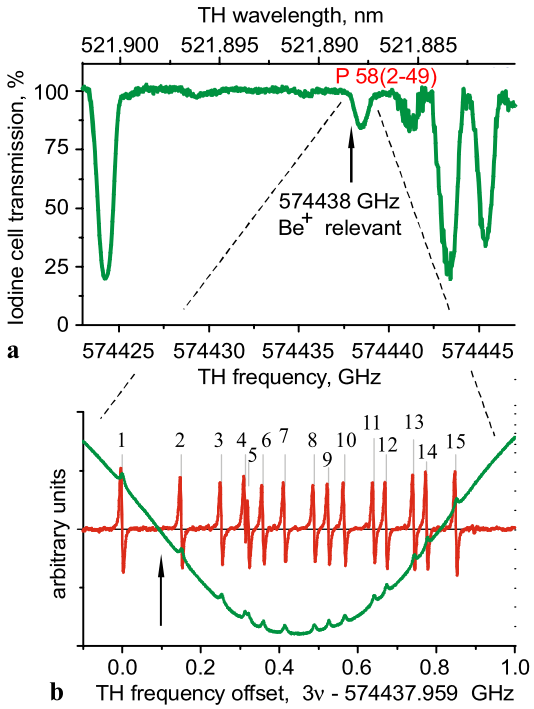

Fig. 5 (**a**) Absorption spectrum of molecular iodine in the range relevant for the Be^+ laser cooling applications (15 cm long iodine cell at 10°C). (**b**) A sub-Doppler survey of the absorption line at 521.888 nm (15 cm long iodine cell at 30°C). Doppler background with hfs Lamb dips (*green*) and the demodulated error signal (*red*)

Figure 5b, red line illustrates the Doppler-free FMTS signal of this convenient line. The green line in the plot shows the Lamb dips of the hfs components on the Doppler background. The P58 line is relatively weak. Therefore the iodine cell was kept at 30°C temperature in order to increase the population of the ground level and, as a result, to improve signal to noise ratio of the generated FMTS error signals.

We determined the absolute frequencies of the hfs components using a femtosecond frequency comb. It is based on a Ti:Sapphire laser (Femtosource Scientific 200) and a commercial comb kit (MenloSystems, FC 8004), modified in-house. The frequency comb's repetition rate and the carrier envelope frequency were locked to an active hydrogen maser (Vremya-Ch), itself steered to GPS on long time scales. The master laser was locked to a particular hfs component. The 1565 nm fundamental wave of the setup was superimposed with the comb on a beat line. The heterodyne beat note between the laser wave and the nearest comb mode was detected with a low-noise photodetector. The detected beat note was filtered, amplified by a tracking oscillator and measured by means of a dead-time-free frequency counter. The results of the measurements are summarized in Table 1. The estimated uncertainty of the frequency values is about 500 kHz as we did not take into account various systematic effects.

The frequency stability of the source was characterized when the master laser was locked to the a1 hfs component. The Allan deviation of the laser frequency is shown in Fig. 6 and the insert shows the beat signal scatter during 1-hour measurement. The Allan deviation of the laser frequency is below 1 kHz for integration times between 2 and 40 seconds. The linear drift (approx. 18 Hz/s) is attributed mainly to the DC offset variation of the locking electronics. It can be removed by temperature stabilization of the critical electronic components (RF mixer, input amplifier). The instability of the iodine cell temperature results in fluctuations of the laser frequency on a time scale of few hundred seconds.

Table 1 Frequencies of the hfs components of the P58(2-49) molecular iodine absorption line. The estimated uncertainty of the frequency values is 500 kHz

hfs line	Freq. (GHz)	hfs line	Freq. (GHz)	hfs line	Freq. (GHz)
a1	574437.959	a6	574438.318	a11	574438.600
a2	574438.110	a7	574438.373	a12	574438.631
a3	574438.212	a8	574438.448	a13	574438.702
a4	574438.273	a9	574438.485	a14	574438.735
a5	574438.281	a10	574438.525	a15	574438.809

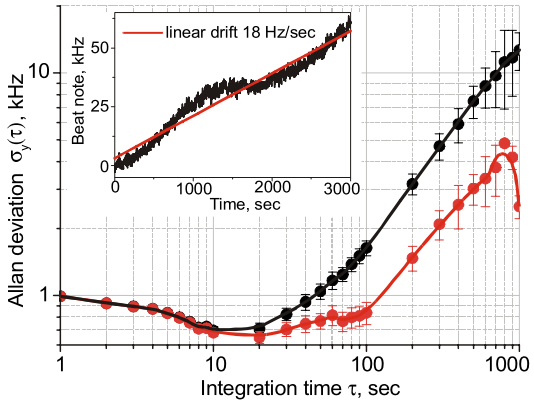

Fig. 6 Allan deviation of the frequency of the master laser (15665 nm) stabilized to the a1 hfs component. *Black*: the deviation is calculated with the linear drift taken into account, *red*: the linear drift is removed. *Inset*: the beat signal scatter

The long-term drift, 250 kHz over 1 h at 313 nm, is much less than the natural linewidth of the Be^+ cooling transition. For Be^+ laser cooling, the frequency of the source can be stabilized using the hfs components of the P58(2-49) iodine transition as a reference. The gap between an iodine reference frequency and a desired frequency can be bridged by the double-pass AOM frequency shifter. The spacing between hfs components (30–150 MHz) is within the bandwidth of the frequency shifter (200 MHz). Hence the UV output wavelength of the source can be precisely set and adjusted over a 1.5 GHz range.

4 Application of the UV source to laser cooling of Be^+

The UV source was developed with the goal of a reliable source for laser cooling of beryllium. Thus, it was tested using our apparatus for laser cooling of Be^+ ions and sympathetic cooling of molecular ions. Details of the setup and the method to obtain trapped laser-cooled Be^+ ions are described in [3]. In brief, we trap a few thousand Be^+ ions in a linear quadrupole radio-frequency trap driven at 14 MHz. The trap is enclosed in a UHV chamber kept below 10^{-10} mbar. To load Be^+ ions into the trap, atoms are thermally evaporated from a beryllium wire, and ionized by an electron beam. Ensembles of Be^+ ions can be brought to temperatures of ≈10 mK by Doppler laser cooling at 313 nm. At these temperatures, the beryllium ions arrange themselves in an ordered state referred to as a Coulomb crystal. The fluorescence of Be^+ ions at 313 nm is monitored by a photomultiplier tube and by a CCD camera.

The UV source was operated at 10–20 mW output power, a typical level for our Be^+ cooling setup. The source was locked to the most red-shifted hfs component (a1) of the P58 transition during the loading of the Be^+ ions into the trap. That corresponds to ≈1 GHz red detuning from the central frequency of the cooling transition and allows for more efficient cooling of hot ions. Subsequently, the UV frequency was tuned toward the cooling transition frequency. We observed the crystallization of the Be^+ ions cloud when the source's frequency was locked to the a4–a8 hfs components.

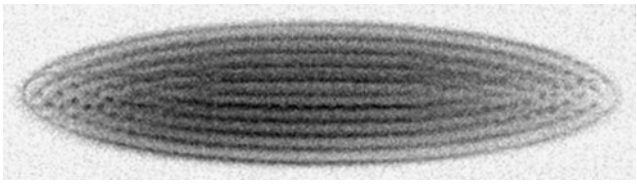

Fig. 7 CCD image of a Be^+ ion crystal

The $^2S_{1/2}$ ground state of the $^2S_{1/2} \leftrightarrow {}^2P_{3/2}$ cooling transition has a hyperfine splitting of 1.25 GHz. The excited $^2P_{3/2}$ state can decay into either of the two hyperfine levels of the ground state. Therefore a 'repumper' laser wave, with the frequency detuning of 1.25 GHz from the 'main' wave is required for more efficient laser cooling. The repumper sidebands in the source's UV output were produced by phase modulation of the master laser at the fundamental wavelength (LO2 in Fig. 1).

An example of a generated Be^+ ion crystal is illustrated in Fig. 7. A characteristic shell-like structure can be clearly seen in the image.

5 Conclusion

In conclusion, we developed a complete setup for generation, frequency stabilization, and precision tuning of UV laser radiation at 313 nm. We tested the source by demonstration of successful laser cooling of Be^+ ions in our ion-trap apparatus.

The setup includes a compact nonlinear frequency conversion stage for quintupling of the high-power IR output of the fiber amplifier seeded by a low-power narrow-linewidth telecom master laser at 1565 nm. The output power of the source at 313 nm is 100 mW when pumped with 15 W at the 1565 nm fundamental wavelength.

The frequency stabilization stage allows for locking the master laser to hfs components of molecular iodine via the third-harmonic output of the source at 522 nm. The source's frequency is fine-tunable by an acoustooptic frequency shifter. We measured the frequencies of the hfs components of P58(2-49) transition in molecular iodine, relevant for Be^+ laser cooling application. The use of iodine as frequency reference means that the source can be operated without the need of a wavelength meter. The frequency stability of the source is, by a considerable margin, sufficient for Be^+ laser cooling.

Features of the source are compactness, robustness, usability, an important use of reliable fiber-optic components.

The source can be transported from one lab to another and reconnected to the fiber laser and to the electronics rack in a matter of minutes. Only little adjustments of the optical setup are required after the transportation because all frequency conversion stages but one are single-pass. The warm-up time is short, about an hour.

With such properties, the source can become a workhorse for laser cooling of Be^+ and similar applications, such as the measurement of linewidths of atomic transitions. A significant amount of source's output at the intermediate wavelengths (1565 nm, 783 nm, 522 nm) remains available. This can be used for other applications; in particular, the third-harmonic output (1 W at 522 nm) can be frequency doubled to produce 260 nm, which is often needed for (non-resonant) photodissociation of atoms or molecules, e.g. in our own experiments on spectroscopy of HD^+. Thus, the UV source becomes multi-purpose. Possible improvements are active stabilization of the UV output power and increased frequency stability.

The developed setup can be used as a building block for a more sophisticated multi-wavelength UV source for cooling of ions into the quantum ground state of motion in an ion trap using the Raman sideband cooling technique [20].

Acknowledgement This research is partly supported by the Deutsche Forschungsgemeinschaft DFG within the project SCHI 431/13-1.

References

1. C. Langer, R. Ozeri, J.D. Jost, J. Chiaverini, B. DeMarco, A. Ben-Kish, R.B. Blakestad, J. Britton, D.B. Hume, W.M. Itano, D. Leibfried, R. Reichle, T. Rosenband, T. Schaetz, P.O. Schmidt, D.J. Wineland, Phys. Rev. Lett. **95**, 060502 (2005)
2. T. Rosenband, D.B. Hume, P.O. Schmidt, C.W. Chou, A. Brusch, L. Lorini, W.H. Oskay, R.E. Drullinger, T.M. Fortier, J.E. Stalnaker, S.A. Diddams, W.C. Swann, N.R. Newbury, W.M. Itano, D.J. Wineland, J.C. Bergquist, Science **319**, 1808 (2008)
3. P. Blythe, B. Roth, U. Fröhlich, H. Wenz, S. Schiller, Phys. Rev. Lett. **95**, 183002 (2005)
4. J.C.J. Koelemeij, B. Roth, A. Wicht, I. Ernsting, S. Schiller, Phys. Rev. Lett. **98**, 173002 (2007)
5. B. Roth, U. Fröhlich, S. Schiller, Phys. Rev. Lett. **94**, 053001 (2005)
6. T. Nakamura, M. Wada, K. Okada, A. Takamine, Y. Ishida, Y. Yamazaki, T. Kambara, Y. Kanai, T.M. Kojima, Y. Nakai, N. Oshima, A. Yoshida, T. Kubo, S. Ohtani, K. Noda, I. Katayama, V. Lioubimov, H. Wollnik, V. Varentsov, H.A. Schuessler, Phys. Rev. A **74**, 052503 (2006)
7. W. Nörtershäuser, D. Tiedemann, M. Žáková, Z. Andjelkovic, K. Blaum, M.L. Bissell, R. Cazan, G.W.F. Drake, Ch. Geppert, M. Kowalska, J. Krämer, A. Krieger, R. Neugart, R. Sánchez, F. Schmidt-Kaler, Z.-C. Yan, D.T. Yordanov, C. Zimmermann, Phys. Rev. Lett. **102**, 062503 (2009)
8. H. Schnitzler, U. Fröhlich, T.K.W. Boley, A.E.M. Clemen, J. Mlynek, A. Peters, S. Schiller, Appl. Opt. **41**, 7000 (2002)
9. A. Tünnermann, T. Schreiber, F. Röser, A. Liem, S. Höfer, H. Zellmer, S. Nolte, J. Limpert, J. Phys. B, At. Mol. Opt. Phys. **38**, S681 (2005)
10. Y. Jeong, J. Nilsson, J.K. Sahu, D.N. Payne, R. Horley, L.M.B. Hickey, P.W. Turner, IEEE J. Sel. Top. Quantum Electron. **13**, 546 (2007)
11. A. Henderson, R. Stafford, Opt. Express **14**, 767 (2006)
12. M. Vyatkin, A. Dronov, M. Chernikov, S.V. Popov, J.R. Taylor, D.V. Gapontsev, V.P. Gapontsev, in *Conference on Lasers and Electro-Optics/Quantum Electronics and Laser Science and Photonic Applications Systems Technologies, Technical Digest (CD)* (Optical Society of America, Washington, 2005), paper CThZ6
13. T. Sudmeyer, Y. Imai, H. Masuda, N. Eguchi, M. Saito, S. Kubota, Opt. Express **16**, 1546 (2008)
14. S. Vasilyev, S. Schiller, A. Nevsky, A. Grisard, D. Faye, E. Lallier, Z. Zhang, A.J. Boyland, J.K. Sahu, M. Ibsen, W.A. Clarkson, Opt. Lett. **33**, 1413 (2008)
15. R. Thompson, M. Tu, D. Aveline, N. Lundblad, L. Maleki, Opt. Express **11**, 1709 (2003)
16. R.W.P. Drever, J.L. Hall, F.V. Kowalski, J. Hough, G.M. Ford, A.J. Munley, H. Ward, Appl. Phys. B **31**, 97 (1983)
17. E.D. Black, Am. J. Phys. **69**, 79 (2001)
18. A. Arie, S. Schiller, E.K. Gustafson, R.L. Byer, Opt. Lett. **17**, 1204 (1992)
19. S. Gerstenkorn, P. Luc, *Atlas du Spectre D'absorption de la Molécule D'iode* (Laboratoire Aimé Cotton, CNRS II, Paris, 1978)
20. M.D. Barrett, B. DeMarco, T. Schätz, V. Meyer, D. Leibfried, J. Britton, J. Chiaverini, W.M. Itano, J.D. Jost, B. Jelenkovic, C. Langer, T. Rosenband, D.J. Wineland, Phys. Rev. A **68**, 042302 (2003)